Journal of Zhejiang University-SCIENCE A
www.jzus.zju.edu.cn; www.springer.com/journal/11582
E-mail: jzus_a@zju.edu.cn

Research Article
https://doi.org/10.1631/jzus.A2600363

Magnetically controlled capsule robot for dual-target constant-rate drug delivery and stable anchoring

Shengqian QU[1,3*], Siyuan HAN[2*], Zitong LIAO[1], Wenbo ZHOU[1], Congxin JIE[1], Chunying LI[3], Shichao NIU[4], Gang LIU[2], Shuxiang GUO[3,6,7], Fanhong CHEN[5✉], Xiaohui DU[5✉], Yang ZHAO[1✉]

[1]*School of Intelligent Manufacturing (Pen-Tung Sah Institute of Micro-Nano Science and Technology), Xiamen University, Xiamen 361102, China*
[2]*School of Public Health, Xiamen University, Xiamen 361102, China*
[3]*Advanced Institute for Ocean Research, Southern University of Science and Technology, Shenzhen 518055, China*
[4]*College of Bionic Science and Engineering, Jilin University, Changchun 130012, China*
[5]*Sensor and Network Control Center, Instrumentation Technology and Economy Institute, Beijing 100055, China*
[6]*Department of Electronic and Electrical Engineering, Southern University of Science and Technology, Shenzhen 518055, China*
[7]*Aerospace Center Hospital, School of Life Science and the Key Laboratory of Convergence Medical Engineering System and Healthcare Technology, Ministry of Industry and Information Technology, Beijing Institute of Technology, Beijing 100081, China*

Abstract: Gastrointestinal (GI) drug delivery remains challenging because sustained constant-rate infusion and positional stability are difficult to achieve simultaneously. Conventional magnetic capsules often rely on burst-type or nonlinear release mechanisms. To address these limitations, a magnetically controlled dual-target constant-rate drug delivery capsule system (M-DCDC) is presented. The system enables highly linear and quantitatively adjustable drug infusion through specialized screw–piston transmission. This mechanism establishes a direct relationship between the magnetic rotation frequency and the delivery rate, achieving a maximum flow rate of 0.1 mL/s with predictable dosage control. Sequential dual-target delivery is achieved through functional decoupling. By reversing the direction of the magnetic field, two independent reservoirs, each with a volume of 0.6 mL, can be selectively actuated at separate target sites. To resist intestinal peristalsis, a self-locking mechanical anchoring module is integrated to maintain positional stability without continuous power consumption. Analytical modeling, finite element analysis (FEA), benchtop tests, and ex vivo experiments using porcine intestines demonstrate that M-DCDC can withstand a peristaltic force of 0.32 N while achieving localized staining. By combining stable anchoring with decoupled constant-rate infusion, the proposed system offers an effective engineering approach for targeted treatment of multifocal GI diseases.

Key words: Capsule robot; Magnetic actuation; Targeted drug delivery; Active anchoring

1 Introduction

Gastrointestinal (GI) diseases often exhibit multifocal involvement and chronic progression, and effective treatment frequently depends on achieving sufficiently high local drug concentrations. These characteristics pose substantial challenges for existing drug delivery strategies (Chu and Traverso, 2022). Although conventional oral preparations cause less discomfort, they often fail to maintain effective drug levels at target sites because of gastric degradation, enzymatic breakdown, and variable intestinal absorption (Hua, 2020). Systemic administration via intravenous injection can bypass some absorption barriers but is commonly associated with off-target exposure and dose-limiting adverse effects (Ezike et al., 2023). These limitations have stimulated growing interest in device-assisted approaches for localized GI drug delivery.

Among these approaches, magnetically controlled capsule systems have gradually evolved from a diagnostic modality into a multifunctional platform capable of integrating imaging and therapeutic functions (Chen et al., 2022; Cao et al., 2024). Recent studies have explored the incorporation of drug delivery modules into

✉ Fanhong CHEN, cfh@tc124.com
Xiaohui DU, dxh@instrnet.com
Yang ZHAO, zhaoy@xmu.edu.cn
* The two authors contributed equally to this work
Yang ZHAO, https://orcid.org/0000-0002-6386-2586

Received June 6, 2026; Revision accepted July 1, 2026; Crosschecked July 31, 2026

© Zhejiang University Press 2026

capsule systems to improve the spatial control of drug administration (Fu et al., 2022; Yang et al., 2025). From a drug delivery perspective, existing magnetically actuated capsule systems still face several practical limitations, including limited controllability of release rates, insufficient capacity for delivery to spatially distinct sites, and unstable positioning under intestinal fluid dynamics and peristalsis.

Regarding drug delivery mechanisms, current systems remain limited in their ability to achieve precise, sustained, constant-rate infusion. Passive approaches, including chemically triggered systems and soft-body deformation-based mechanisms (Esendag et al., 2024), typically exhibit nonlinear release profiles characterized by rapid initial release followed by a gradual decline in release rate (Sun et al., 2023). Such time-dependent release behavior complicates dose prediction and limits their suitability for dose-sensitive therapies (Cai et al., 2024). Although active mechanisms based on springs, torsional elements (Cao et al., 2025), or shape-memory alloys can provide mechanical actuation, they often operate in a discrete or burst-like manner rather than enabling sustained and adjustable flow control (Zheng et al., 2023; Zhang et al., 2025). In addition, capsule systems originally designed for fluid sampling may generate insufficient or poorly regulated driving pressure, further restricting their applicability to controlled drug infusion (Wu et al., 2025).

Beyond release-rate control, spatially selective drug delivery remains a major challenge for magnetic capsule systems, as most existing designs support only single-drug, single-target operation. Although multi-chamber capsules can increase payload capacity (Valdastri, 2025), the lack of effective functional decoupling limits the independent control of multiple drug compartments (Li et al., 2025; Ye et al., 2025), making sequential or region-specific dual-drug delivery difficult to achieve (Zheng et al., 2022; Wang et al., 2025). Moreover, intestinal peristalsis and fluid motion can displace capsules during delivery, thereby reducing localization accuracy and reliability. Although sensor fusion and localization algorithms can improve tracking performance (Bianchi et al., 2022; Zhang H et al., 2022; Zhang P et al., 2024), they do not provide physical stabilization (Wang et al., 2021). Existing anchoring approaches either carry a risk of mucosal injury or are difficult to integrate and decouple within the limited capsule volume (Song et al., 2022; Yu et al., 2025). These challenges are further exacerbated by the limited and variable efficiency of wireless power transfer, which restricts the use of high-power or continuously actuated stabilization mechanisms (Wen et al., 2024; Han et al., 2025).

M-DCDC was introduced as a magnetically controlled dual-target constant-rate drug delivery capsule system designed to overcome the critical limitations of conventional GI drug delivery, specifically the lack of rate control and positional instability, as illustrated in Fig. 1. The innovative contributions are as follows:

1. Unlike traditional mechanisms prone to burst-type release, M-DCDC utilizes specialized screw-piston

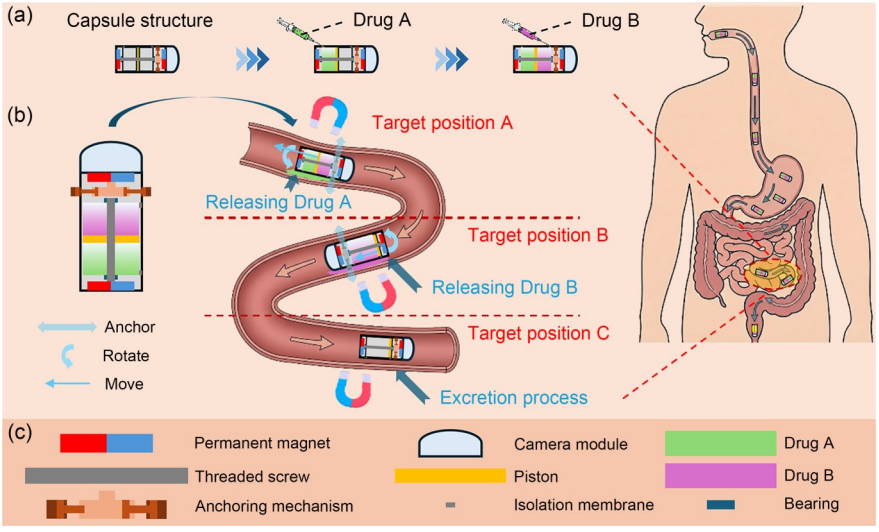


Fig. 1 Structural design, function, and application of M-DCDC: (a) structure of M-DCDC and the drug injection process; (b) schematic illustration of M-DCDC anchoring and multi-target drug release in the intestinal tract (target positions A and B); (c) simplified structural composition of M-DCDC

transmission. This mechanism converts the magnetic rotational frequency into a highly linear and quantitatively adjustable drug infusion, achieving a flow rate of up to 0.1 mL/s.

2. A key advance lies in the functional decoupling of the delivery sequence. By reversing the magnetic field direction, two distinct 0.6 mL reservoirs can be independently actuated, enabling sequential delivery to spatially separated lesions within a single procedure.

3. To ensure stability against peristalsis, the system integrates a mechanical self-locking anchoring module. This module can resist peristaltic forces without requiring continuous power consumption or constant magnetic actuation, thereby improving dosing reliability and localization accuracy.

2 Robot structure design

2.1 M-DCDC

Fig. 2 illustrates the overall structure of the proposed capsule robot. With a diameter of 13 mm and a

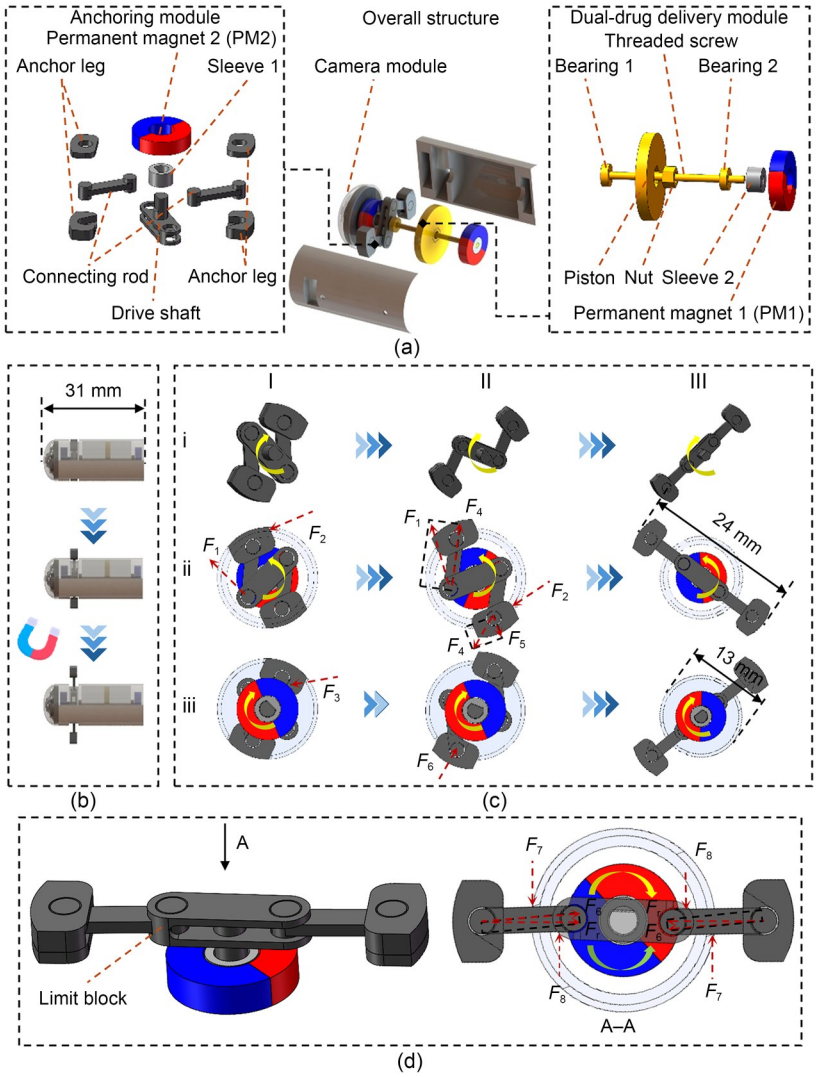


Fig. 2 Design of the M-DCDC: (a) overall structure and detailed design of the M-DCDC; (b) schematic diagram of the M-DCDC unfolding process from the contracted state to the anchored state; (c) kinematics and force principles of the anchoring module: (I) initial contracted state; (II) during the drive-deployment phase, demonstrating the transmission of the link drive force F_1 and the leg radial drive force F_4; (III) fully deployed state; (i) isometric projection view; (ii) rear view; (iii) front view; (d) mechanical self-locking design of the anchoring module. F_1–F_8 represent various forces under different working conditions of the mechanism, and F_r denotes the collinear resultant force produced by two anchoring feet with equal magnitude and opposite directions, which cancel each other out in the deadlock state

length of 31 mm, the capsule is primarily designed for use in the intestinal environment and can be administered orally. Given that the adult esophagus has a diameter of approximately 20 mm and a length of approximately 250 mm, sufficient anatomical space is available for smooth capsule passage. The system integrates three core functional modules: a camera module, an anchoring module, and a drug delivery module. The camera module enables real-time observation of the intestinal environment. The anchoring module employs a linkage mechanism to deploy anchoring legs, enabling reliable fixation of the capsule while minimizing the risk of intestinal wall damage, thereby providing a stable platform for targeted drug delivery. The drug delivery module can accommodate either a single drug reservoir or two separate reservoirs, with a maximum capacity of 1.3 mL for single-drug loading or 0.6 mL per reservoir for dual-drug operation. Under external magnetic actuation, the system enables controlled and adjustable-rate release of one or two drugs. Following drug delivery, the anchoring mechanism can be retracted to restore capsule mobility for subsequent navigation.

It should be noted that the camera module integrated into the current physical prototype serves as a structural and spatial placeholder. Because the primary focus of this study is to validate the mechanical anchoring and dual-drug delivery mechanisms, reserving realistic volume and weight for a standard vision module ensures that the proposed actuation structures can be accommodated within clinically viable capsule dimensions, thereby paving the way for future fully integrated systems.

2.2 Dual-drug delivery module

To achieve multifunctional operation within the limited capsule volume, this study proposes an integrated module based on screw–piston transmission. Positioned at the rear of the robot, the module comprises a radially magnetized permanent magnet (PM1), a lead screw, a piston with an embedded nut, and an isolation membrane. This design uses a single actuation source to generate bidirectional linear motion. PM1 is rigidly attached to the screw and axially supported by bearings. Because the rotation of the piston is constrained by the capsule wall, an external rotating magnetic field drives PM1 to rotate, which in turn rotates the screw and converts rotational torque into axial reciprocating motion of the piston, as shown in Fig. 3. By exploiting the reversibility of the screw–nut mechanism, the direction of piston motion can be controlled by switching the rotation direction of the external magnetic field. This bidirectional capability enables precise, sequential, and selective release of two distinct drugs, thereby improving space utilization and enhancing therapeutic flexibility.

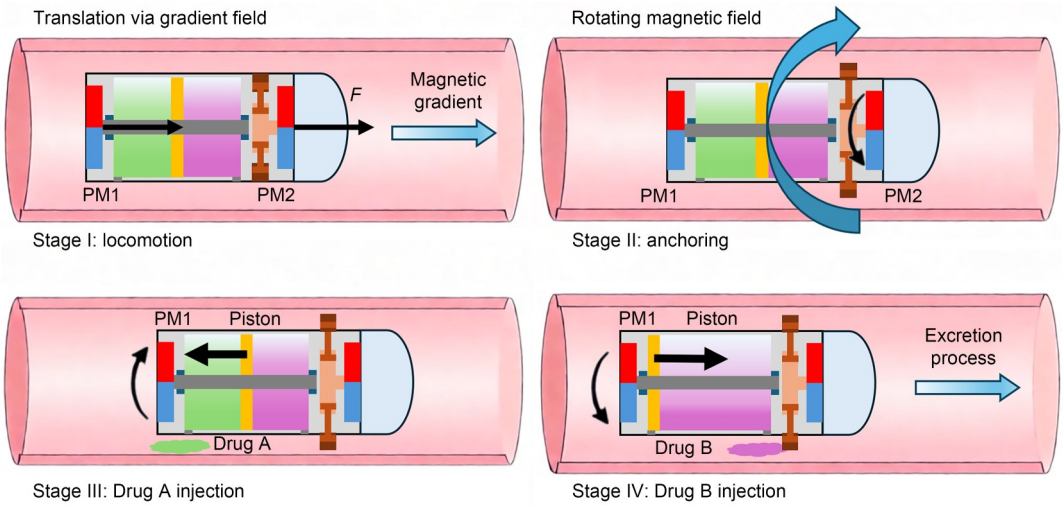


Fig. 3 Dual-drug injection workflow. Stage I: the M-DCDC achieves axial locomotion inside the intestinal tract driven by an external magnetic gradient field (*F* is the traction force exerted by the external magnet on the internal magnet). Stage II: PM2 is rotated by an external magnetic field to activate anchoring. Stage III: PM1 is controlled to rotate clockwise through the external magnetic field, releasing Drug A. By adjusting the rotation speed of the external magnetic field, the drug delivery rate and dosage can be precisely controlled. Stage IV: after re-anchoring, drug delivery to the next lesion site can proceed, releasing Drug B

2.3 Anchoring module

To achieve effective anchoring within a limited space, this study proposes a linkage-based module comprising a central magnetic shaft and telescopic legs. During the cruising phase, the mechanism retracts to a diameter of 13 mm to ensure smooth passage. Upon activation, the magnetic shaft drives the linkages to expand the module to a diameter of 24 mm. The nonlinear relationship between the radial expansion L_{rad} and the rotation angle α enables adaptation to variations in intestinal diameter while converting magnetic torque into an effective radial force F_4. Furthermore, to minimize energy consumption during long-term anchoring, a mechanical self-locking mechanism is implemented. At maximum expansion, the interaction between the intestinal resistance F_6 and the shell support force F_7 creates a counter torque through stop block F_8, ensuring that the anchoring structure remains fully deployed and engaged without an external magnetic field.

3 Analytical model of magnetic fields

3.1 Magnetic control system

The driving force of the capsule robot originates from the interaction between the magnetic field $\boldsymbol{B}$ generated by the external permanent magnet (EPM) and the magnetic moment $\boldsymbol{m}$ of the internal permanent magnet. Similar principles have been applied in navigation systems composed of dual permanent magnets for accurate posture control (Kim et al., 2024). When a rotating magnetic field is applied, the magnetic torque $\boldsymbol{T}$ exerted on the internal permanent magnets (PM1 and PM2) serves as the primary actuation source for the anchoring and lead-screw mechanisms. This torque can be expressed as:

$$\boldsymbol{T}=\boldsymbol{m}\cdot\boldsymbol{B}=|\boldsymbol{m}||\boldsymbol{B}|\sin\theta\cdot\boldsymbol{n}, \tag{1}$$

where θ is the angle between the magnetic moment and the external magnetic field, and $\boldsymbol{n}$ is the unit normal vector perpendicular to both $\boldsymbol{m}$ and $\boldsymbol{B}$, indicating the direction of the magnetic torque.

When a gradient magnetic field is applied, the magnetic force $\boldsymbol{F}$ driving the capsule's cruising motion is expressed as:

$$\boldsymbol{F}=(\boldsymbol{m}\cdot\nabla)\boldsymbol{B}. \tag{2}$$

Based on the aforementioned model, a simulation analysis of the magnetic drive system was performed using COMSOL Multiphysics software. The grades and dimensions of the permanent magnets were selected by considering the required actuation torque, magnetic decoupling, and spatial constraints. PM1 and PM2, which are embedded inside the capsule, were selected as N35 magnets to provide sufficient torque for drug delivery and anchoring while reducing undesired magnetic coupling between the two internal magnets. PM3 was selected as an N52 magnet to compensate for the rapid decay of magnetic field strength with distance and to ensure sufficient actuation capability within the working space. To provide a comprehensive understanding of the magnetic interactions, Fig. 4 presents both quantitative characteristic curves and the corresponding finite element analysis (FEA) heatmaps.

Figs. 4b and 4c visualize the magnetic flux density distribution when the external magnet (PM3) is placed at different vertical distances along the *Y*-axis. These field maps are consistent with the nonlinear decay of the magnetic coupling torque experienced by PM1 and PM2, as quantified by the characteristic curves in Fig. 4d. Similarly, Figs. 4g–4i illustrate the dynamic spatial variations in the magnetic field as PM3 translates along the *X*-axis. These field distributions explain the transitions between the attractive and repulsive forces acting on the capsule, which directly correspond to the force variations plotted in Fig. 4e. Together, the theoretical analysis and field visualization confirm the feasibility of the proposed magnetic drive scheme within the effective workspace.

3.2 Dual-drug delivery analysis

To estimate the driving force required for controlled drug infusion and to guide the design of the release mechanism, the flow behavior of liquid or weakly viscous drug formulations within the microneedle was modeled using the Poiseuille flow equation. Under the assumption of steady, laminar flow in a cylindrical needle, the relationship between the volumetric flow rate Q and driving pressure difference ΔP can be expressed as:

$$\Delta P=\frac{8\eta LQ}{\pi r^4}, \tag{3}$$

where $\Delta P=p_2-p_1$ represents the pressure difference required to overcome fluid resistance (p_2 is the driving pressure within the cavity, and $p_1\approx0$ is the ambient

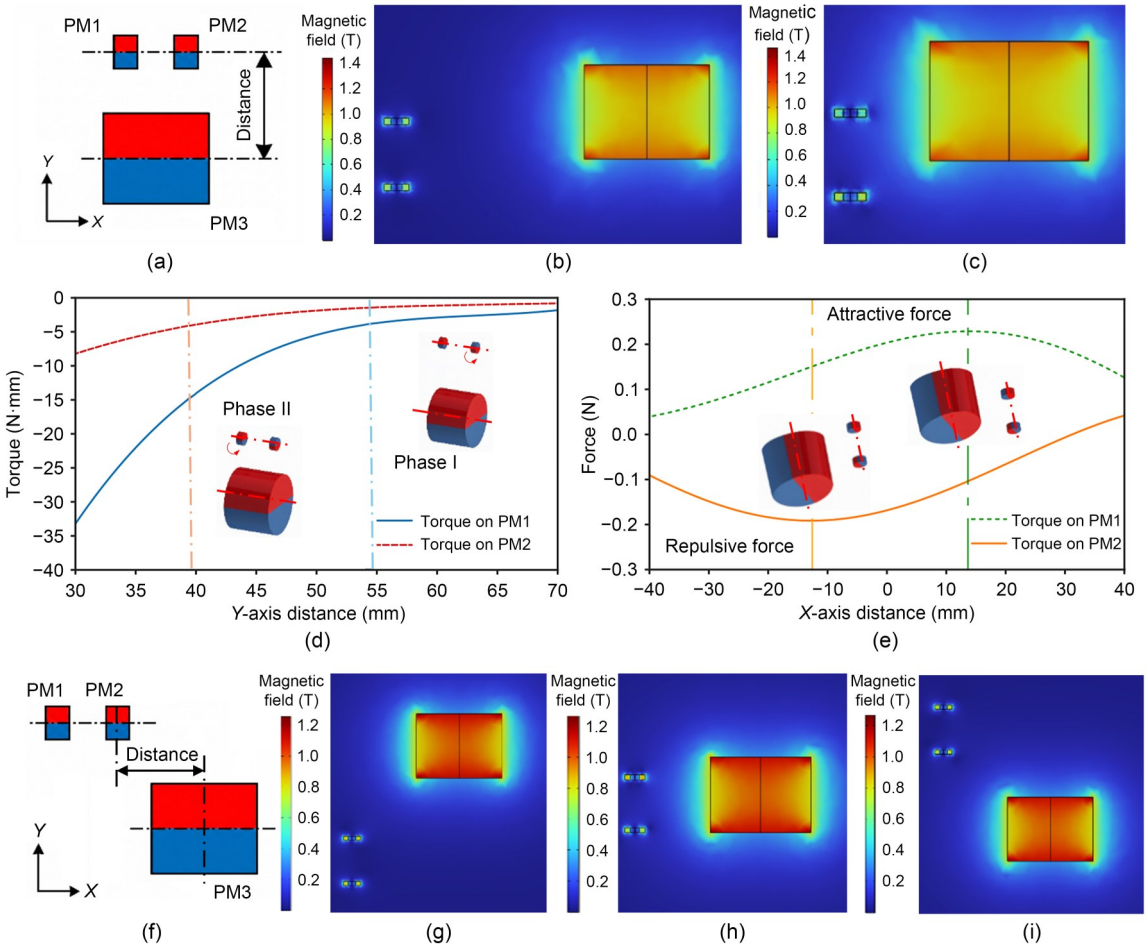


Fig. 4 Simulation analysis and characterization of magnetic drive systems: (a) schematic of the simulation model showing the external magnet (PM3) moving along the *Y*-axis; (b) and (c) FEA heatmaps at different *Y*-axis positions; (d) calculated characteristic curve of magnetic coupling torque versus distance, indicating torque decay trends at different stages; (e) variation curve of magnetic driving force with *X*-axis displacement; (f) schematic diagram of the simulation model with the external magnet moving along the *X*-axis; (g)–(i) magnetic field distribution maps at different positions along the motion path

pressure in the intestinal tract), η denotes the dynamic viscosity of the drug, L is the length of the injection needle, and r is the inner radius.

In the proposed screw–piston drive mechanism, the volumetric flow rate Q is geometrically related to the linear advancement velocity v_{piston} of the piston and the effective cross-sectional area of the working chamber A_{chamber}, $Q=v_{\text{piston}}\cdot A_{\text{chamber}}$. The linear velocity of the piston is directly related to the angular velocity ω of the external magnet through the lead P_{h} of the screw:

$$v_{\text{piston}}=\frac{\omega}{2\pi}P_{\text{h}}. \tag{4}$$

By combining the above equations, a linear mapping relationship can be established between the rotational frequency and the drug flow rate Q:

$$Q(\omega)=A_{\text{chamber}}\frac{P_{\text{h}}}{2\pi}\cdot\omega. \tag{5}$$

This relationship indicates that, for a given mechanical configuration and drug viscosity, the infusion rate is proportional to the rotational speed of the external magnetic field. Provided that the magnetic torque is sufficient to generate the piston thrust $F_{\text{thrust}}=\Delta P\cdot A_{\text{chamber}}$, the release rate and delivered dose can be adjusted in a predictable manner by modulating ω, offering a continuous alternative to discrete, switch-based magnetic actuation strategies.

3.3 Anchoring analysis

To prevent the capsule from being swept away by intestinal peristalsis during its mission, it is essential

to ensure that the axial resistance F_{anchor} generated by the anchoring mechanism exceeds the maximum peristaltic force $F_{\text{peristalsis}}$ of the intestine. According to relevant physiological studies, the axial peristaltic force density in the small intestine is approximately 17.2 g/cm (Miftahof, 2005). For a capsule robot of length L_{cap}, the maximum peristaltic thrust can be estimated as:

$$F_{\text{peristalsis}} \approx 17.2 \times 10^{-3} \times L_{\text{cap}} \times g, \tag{6}$$

where g is the gravitational acceleration (9.8 m/s^2).

Based on the length and weight of this capsule, this force is approximately 0.32 N. After the anchoring legs extend, they compress the intestinal wall, with the resulting anchoring force primarily composed of friction. Let the radial support force exerted by the anchoring legs on the intestinal wall be F_{r}. According to Coulomb's friction law, the anchoring resistance F_{anchor} is:

$$F_{\text{anchor}} = \mu_{\text{c}} \cdot \sum F_{\text{r}}, \tag{7}$$

where μ_{c} is the friction coefficient of intestinal mucosa.

In this study, the equivalent friction coefficient between the capsule anchoring legs and the intestinal mucosa was estimated to be approximately 0.08–0.20 based on existing biomechanical evaluations of ex vivo porcine intestinal tissues (Kim et al., 2006). For the theoretical estimation and numerical simulation, a friction coefficient of 0.2 was adopted to evaluate the anchoring reliability.

To ensure delivery stability, the system design must satisfy the following mechanical conditions:

$$F_{\text{anchor}} > F_{\text{peristalsis}}. \tag{8}$$

A simulation analysis of the anchoring device was performed using Ansys software, as shown in Fig. 5. First, the stress and strain distributions under the self-locking state of the linkage mechanism were evaluated, and the corresponding stress–strain relationship was analyzed. Second, the stress condition induced by intestinal peristalsis was investigated. The contact area of each anchoring foot was approximately 10 mm^2. Based on the FEA simulation results under the maximum mechanical self-locking state, the anchoring mechanism exerts a total radial support force (F_{r}) of approximately 2.4 N against the intestinal wall without causing mucosal damage. Taking the estimated mucosal fiction coefficient (μ=0.2), the theoretical maximum axial anchoring resistance is calculated as $F_{\text{anchor}} = \mu_{\text{c}} \cdot \sum F_{\text{r}} = 0.48$ N. This result exceeds the maximum estimated peristaltic force (0.32 N), thereby satisfying the stability condition defined in Eq. (8).

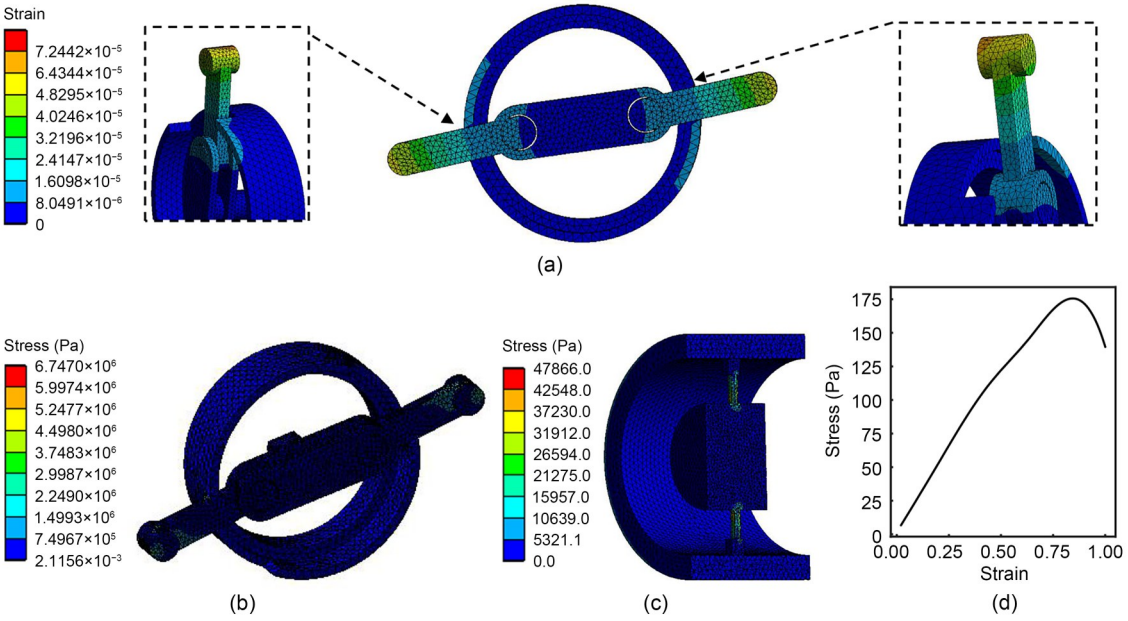


Fig. 5 Mechanical simulation performance evaluation of the anchoring mechanism: (a) strain distribution contour at the maximum deployment, highlighting critical connection points; (b) stress distribution contour at the maximum deployment; (c) stress at the time of capsule anchoring during intestinal peristalsis; (d) stress–strain characteristic curves of the anchoring mechanism

4 Experiments

4.1 Prototyping

To experimentally validate the proposed design, a physical prototype (Φ13.0 mm×31.5 mm) was fabricated, as shown in Fig. 6. The capsule shell and internal supports were manufactured via high-precision stereolithography appearance (SLA) 3D printing. The internal mechanism integrates a custom-machined brass lead screw (P_h=0.35 mm) with radially magnetized permanent magnets for precise actuation, while a highly elastic thermoplastic elastomer (TPE) film serves as an isolation barrier for the drug storage module. To withstand the gastrointestinal environment, this component is bonded using medical-grade adhesive to prevent leakage.

In the absence of applied pressure, the isolation membrane maintains a microscopic orifice that effectively prevents drug leakage. When the drug chamber is subjected to an outward positive pressure, this orifice expands, allowing for proper drug release. Conversely, under inward negative pressure, the orifice also expands slightly. However, owing to the relatively high viscosity of the intestinal fluid, fluid ingress is minimal. Consequently, this design reduces fluid backflow into the drug reservoir, as illustrated in Fig. 6i.

4.2 Decoupling height test

To characterize the operational separation between the anchoring and drug delivery modules, decoupling tests were conducted to map the effective magnetic workspace based on magnetic field attenuation with height and the distinct torque requirements of each module. As shown in Figs. 6c and 6d, the anchoring module requires a relatively low operating height to generate sufficient magnetic torque to overcome the mechanical resistance of the linkage mechanism. In contrast, the drug delivery module, which incorporates low-friction bearings, can be actuated under reduced magnetic torque.

These measurements reveal a separation in the height-dependent actuation thresholds of the two modules, which can be exploited for selective control.

Based on the experimentally identified thresholds, a sequential control strategy was implemented. In this strategy, the external magnet is first positioned at a lower height to activate the anchoring mechanism and is subsequently raised to a higher position to actuate the drug delivery piston while maintaining the anchored state. The results demonstrate that modulation of the external magnet height provides a feasible approach for achieving functional decoupling between anchoring and drug delivery under the tested conditions.

4.3 Magnetic model validation

To experimentally examine the validity of the magnetic torque model, a dedicated torque measurement platform was constructed, as shown in Figs. 6e and 6f. The capsule prototype was rigidly mounted on a high-precision dynamic torque sensor, while the external permanent magnet was positioned at different distances ranging from 4.0 to 7.0 cm. At each distance, the peak magnetic coupling torque was recorded, and five independent measurements were performed to obtain the mean value.

Fig. 6h compares the experimentally measured torque values with the theoretical predictions obtained from the magnetic simulation model. The experimental results show close agreement with the simulated curve and remain within the 95% confidence interval (CI) across the tested distance range, indicating good consistency between the model predictions and physical measurements. These results support the applicability of the proposed magnetic model for estimating the available driving torque within the intended operating workspace. In particular, at a representative working distance of 6.0 cm, the measured torque exceeds 0.5 N·mm, providing an adequate actuation margin for subsequent screw-driven drug delivery and anchoring operations under the experimental conditions considered.

4.4 Dual-drug delivery accuracy test

To rigorously evaluate the quantitative control capability of the screw–piston mechanism, a series of bench tests was conducted to validate the relationships among magnetic drive frequency, flow rate, and dosing accuracy, as shown in Fig. 7. The linearity of the drive system was first assessed. As derived from Eq. (5), the drug flow rate is theoretically proportional to the rotational speed of the external magnetic field.

The instantaneous flow rate was measured at different magnetic field frequencies. The results plotted in Fig. 7f demonstrate a highly linear correlation between the input frequency and the output flow rate, with the experimental data closely matching the theoretical model. This confirms that the drug delivery rate

can be precisely modulated by adjusting the rotational speed of the external magnet.

Experiments were performed at three target flow rates: 0.02, 0.05, and 0.10 mL/s to verify the temporal stability of the infusion process. Fig. 7g shows that the cumulative delivered volume increased approximately linearly with time under all tested settings, indicating consistent infusion behavior throughout the delivery duration. Minor fluctuations were observed but remained within a limited range across repeated trials.

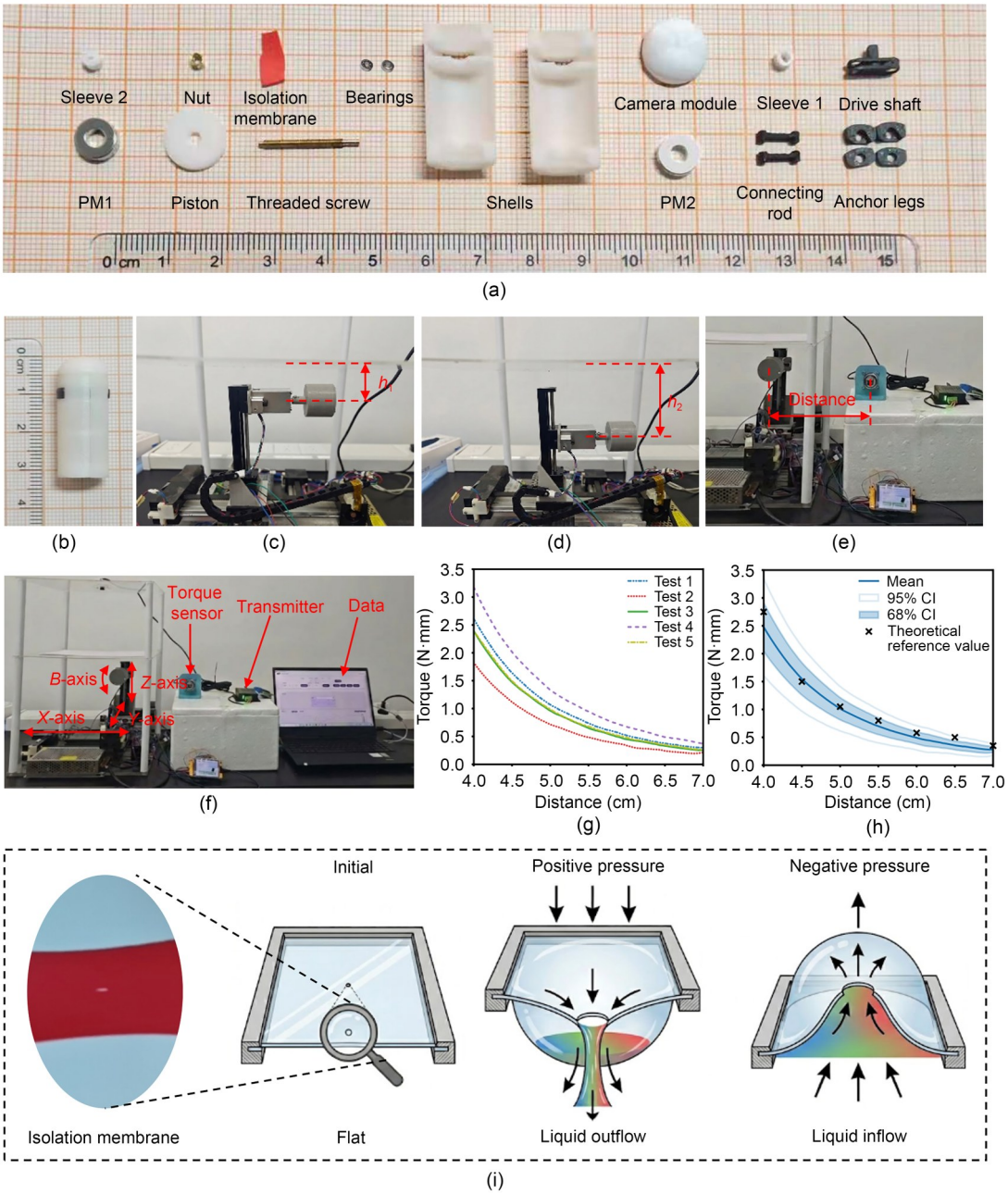


Fig. 6 M-DCDC prototype structure and magnetic drive characteristic testing: (a) and (b) exploded view of the robotic prototype and details of its internal core components; (c) and (d) demonstration of the effective working space, indicating the effective distance range of magnetic control; (e) and (f) schematic of the magnetic drive torque measurement experiment and physical test platform incorporating a torque sensor; (g) raw experimental curves showing magnetic coupling torque decay with distance across five distinct test sequences; (h) statistical analysis of magnetic torque characteristics, presenting comparisons of the average torque curve, confidence interval (CI), and theoretical reference value; (i) working principle of the isolation membrane

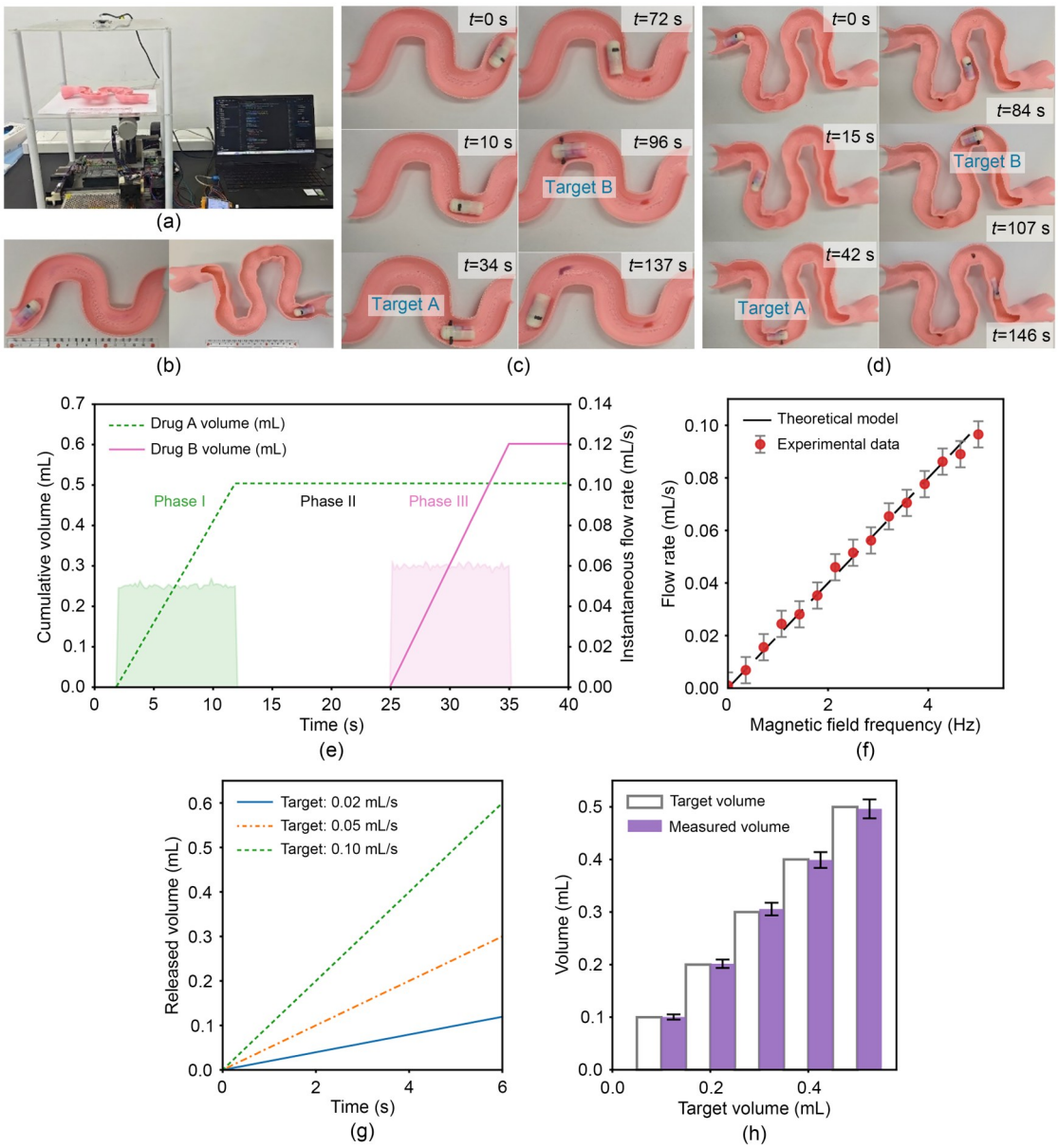


Fig. 7 In vitro evaluation of dual-drug delivery performance: (a) and (b) experimental setup and simulated gastrointestinal model; (c) and (d) time-lapse sequences of the dual-target release process; (e) cumulative release volume showing decoupled control (Phase I: release of Drug A; Phase II: move from target position A to target position B; Phase III: release of Drug B); (f) linear fit between flow rate and magnetic frequency; (g) released volume profiles at different set flow rates; (h) accuracy analysis comparing target versus measured volumes

In addition, dosing accuracy was evaluated by setting target release volumes between 0.1 and 0.5 mL and comparing them with the experimentally measured delivered volumes. The results in Fig. 7h show only small deviations between the target and measured values, with low standard deviations across repeated measurements. These results suggest that the proposed system is capable of repeatable and controllable drug dosing under the tested experimental conditions.

4.5 Anchoring test

Anchoring stability and resistance to intestinal peristalsis were evaluated through ex vivo dragging experiments using freshly harvested porcine intestines, as shown in Fig. 8. The capsule was subjected to controlled axial pulling in both unanchored and anchored configurations, and the resulting resistance forces were recorded for comparative analysis. Deployment of the

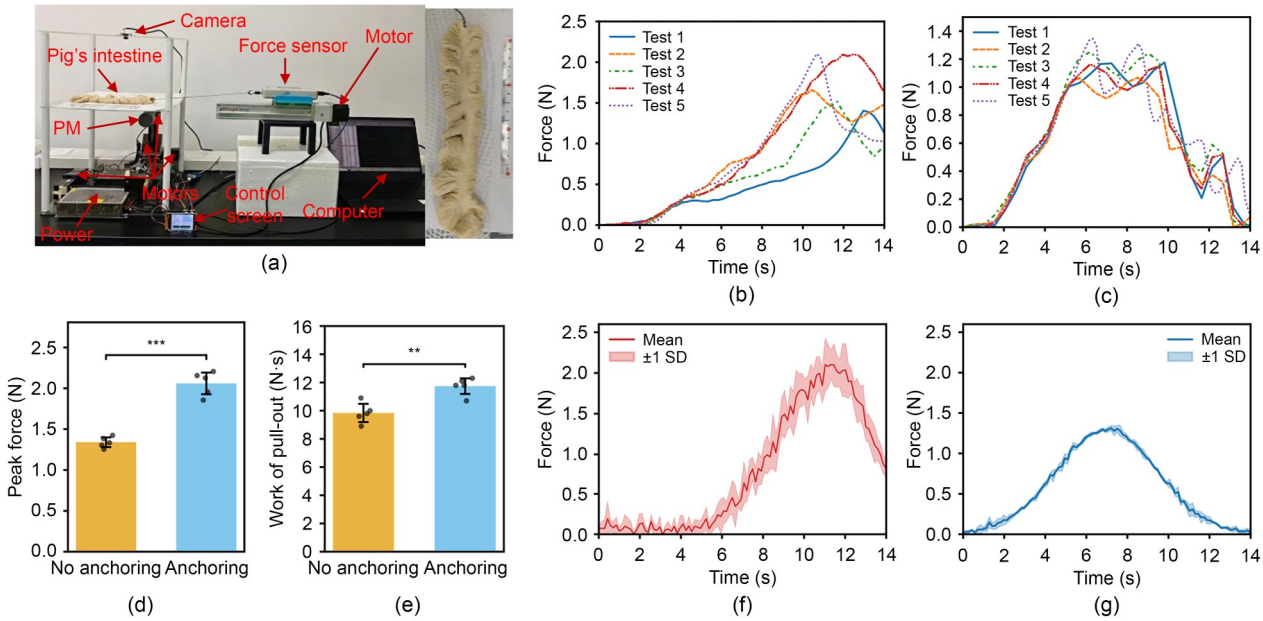


Fig. 8 Mechanical ex vivo performance evaluation of the anchoring mechanism: (a) experimental setup for anchoring force testing on ex vivo porcine intestines; (b) and (c) raw drag force–time curves for five independent trials in anchored and unanchored states, respectively; (d) and (e) statistical comparison of the peak force and work of pull-out ($^{***}p$<0.001, $^{**}p$<0.01), respectively; (f) and (g) mean resistance curves (±SD) comparing anchored and unanchored states, respectively

linkage-based anchoring mechanism resulted in a marked increase in mechanical resistance, primarily arising from frictional interaction with the intestinal folds. Quantitative analysis showed that both the mean peak resistance force and the withdrawal work were significantly higher in the anchored state than in the unanchored state ($^{***}p$<0.001; $^{**}p$<0.01). The measured peak resistance forces fell within the range of peristaltic forces reported in the literature for the small intestine. These findings suggest that the proposed anchoring mechanism can provide enhanced positional stability under physiologically relevant mechanical disturbances during ex vivo testing.

4.6 Ex vivo integrated experiments

Ex vivo integrated experiments were conducted using freshly harvested porcine intestines to evaluate the feasibility of the proposed M-DCDC system under physiologically relevant conditions, as shown in Fig. 9. A sequential operation protocol involving navigation, anchoring, and drug release was implemented. Guided by a gradient magnetic field, the capsule was navigated to the first predefined target location, where the anchoring mechanism was deployed to stabilize the device against the intestinal wall, followed by the release of Drug A through the screw–piston delivery module.

After the first release step, the anchoring mechanism was retracted to restore capsule mobility, and the device was subsequently guided to a second downstream target. The anchoring and drug release procedures were then repeated for Drug B delivery. Visual inspection after the experiments revealed two spatially separated localized staining regions corresponding to the intended release sites. These observations demonstrate that the system can perform sequential multisite drug delivery while maintaining positional separation under ex vivo experimental conditions.

5 Discussion

The proposed M-DCDC system addresses several persistent challenges in gastrointestinal drug delivery that have been widely reported in the literature, including limited control over the release rate, difficulty in achieving spatially separated delivery, and reduced positional stability during drug administration. Rather than introducing a fundamentally new actuation paradigm, this study focuses on the system-level integration of magnetic actuation, mechanical anchoring, and quantitative infusion within a single capsule platform.

As summarized in Table 1, many existing magnetic capsule robots exhibit inherent limitations in drug release controllability. Approaches based on chemical reactions (Esendag et al., 2024) or magnetic torsion springs (Cao et al., 2025) typically rely on threshold-triggered or discrete actuation mechanisms, which limit their ability to provide adjustable and sustained infusion rates. Soft capsule robots driven by ferrofluids or deformable structures have improved compliance and reduced contact stress with intestinal tissue (Hua et al., 2022). However, drug release in these systems is generally governed by deformation or squeezing processes, which can lead to nonlinear release profiles and transient bursts that are difficult to regulate over time. In contrast, the M-DCDC employs a rigid screw–piston transmission mechanism, enabling a direct and predictable

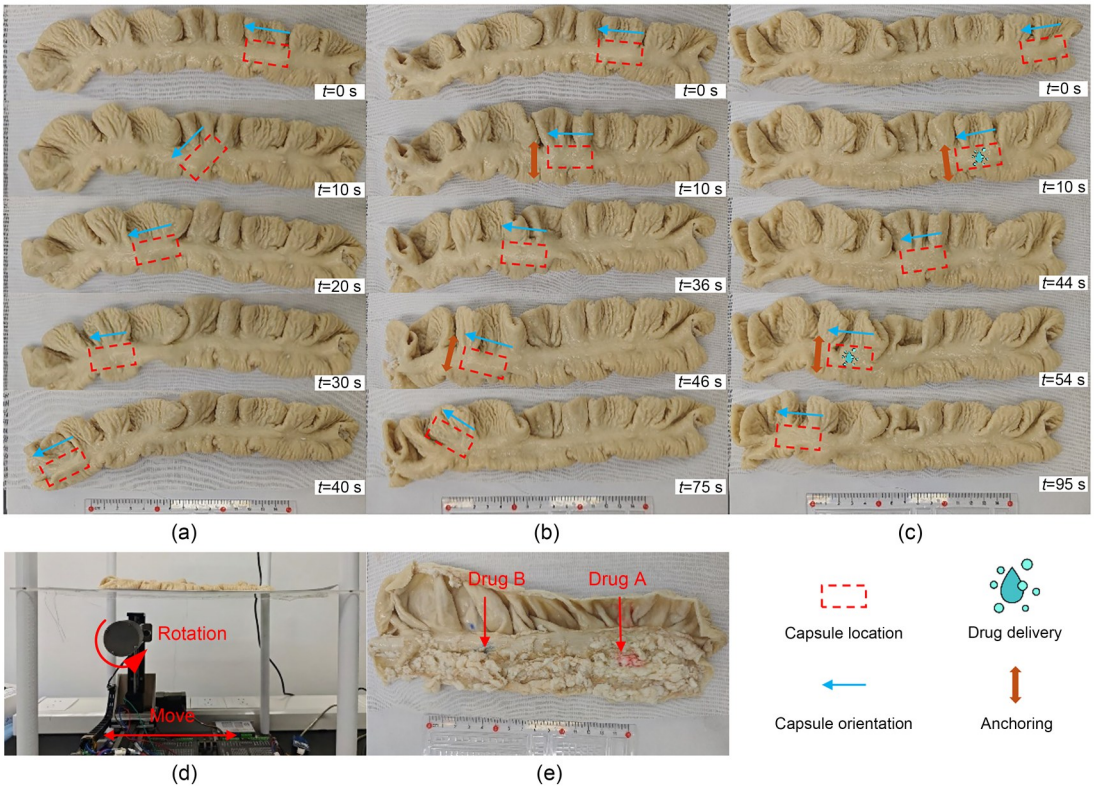


Fig. 9 Ex vivo intestinal integrated experimental validation of the M-DCDC robot: (a) time-series screenshots of capsule movement within the intestine; (b) time-series snapshots of capsule movement and stationary anchoring; (c) time-series snapshots of dual-drug delivery execution; (d) schematic of motion control for the magnetically controlled platform; (e) demonstration of staining effects within the intestine after drug injection

Table 1 Comparison of the proposed robot with related works

Reference	Robot size, $D\times L$ (mm)	Powered by	Anchoring capability	Drug release mechanism	Rate controllability	Quantitative dosage control	Multi-target/ dual-drug
Esendag et al. (2024)	11×26	Chemical reaction	No	Pressure expansion	No	Yes	No
Cao et al. (2025)	14×29	Magnetic field	No	Torsion spring	No	Yes	No
Wu et al. (2025)	9.8×20	Magnetic field	No	Magnetic valve	No	Yes	Yes
Ye et al. (2025)	13×29	Magnetic field	No	Balloon puncture	No	Yes	Yes
Song et al. (2022)	16×50	Magnetic field	Yes	Valve opening	No	Yes	No
Hua et al. (2022)	Soft capsule	Magnetic field	No	Squeeze	No	Yes	No
This study	13×31	Magnetic field	Yes	Screw–piston	Yes	Yes	Yes

relationship between the rotational speed of the external magnetic field and the volumetric flow rate. Although this rigid configuration introduces additional mechanical complexity compared with soft designs, it provides a practical means of achieving adjustable and repeatable release behavior under controlled experimental conditions.

Spatially selective drug delivery presents an additional challenge for capsule-based systems. Although recent work has demonstrated a dual-chamber capsule capable of delivering two drugs, the absence of a dedicated physical anchoring mechanism may limit positional stability during the release window, particularly in the presence of intestinal peristalsis (Ye et al., 2025). Other magnetic capsule systems have addressed stability or tissue interaction through orientation locking (Erin et al., 2021) or origami-inspired mechanisms for biopsy and sampling (Huang et al., 2025). However, these designs do not incorporate actively controlled continuous drug infusion in combination with mechanical stabilization.

The M-DCDC integrates a self-locking mechanical anchoring module with a height-modulated, functionally decoupled dual-drug delivery mechanism, allowing sequential delivery at multiple locations while maintaining positional stability during ex vivo testing. This integrated design demonstrates a feasible pathway for combining localized stabilization and quantitative infusion within the size constraints of a capsule robot, thereby providing a complementary approach to existing soft or purely magnetically stabilized systems.

Despite the promising ex vivo results, several limitations should be noted. The drug flow model and experiments mainly considered liquid or weakly viscous formulations under laminar flow, and higher-viscosity or non-Newtonian drugs may require further characterization. Moreover, ex vivo porcine intestines cannot fully replicate in vivo gastrointestinal dynamics, such as active peristalsis, variable luminal pressure, and long-term tissue responses. In addition, the experiments focused on short-term anchoring and delivery, without assessing prolonged deployment, repeated operating cycles, or potential tissue irritation. Future work should therefore emphasize in vivo studies, long-duration testing, and optimization of the anchoring design and actuation parameters to further evaluate safety, robustness, and clinical feasibility.

Furthermore, although the anchoring mechanism operated smoothly in the clean ex vivo environment, the presence of food residues or complex debris in the in vivo gastrointestinal tract may pose a risk of the anchoring legs becoming stuck during deployment or retraction. Addressing this mechanical reliability issue through optimized leg geometry, anti-adhesive coatings, or redundant retraction mechanisms will be a critical focus of future in vivo studies.

6 Conclusions

This study presents the M-DCDC, a magnetically actuated capsule system that integrates mechanical anchoring with quantitatively controllable and spatially selective drug delivery. By combining a screw–piston transmission mechanism with magnetic actuation, the system enables adjustable-rate infusion and provides an alternative to the burst-type release mechanisms commonly used in passive or spring-based capsule systems. Functional decoupling further enables sequential delivery of two drugs to spatially separated sites within a single capsule platform. In addition, a compact self-locking anchoring mechanism is incorporated to enhance positional stability during drug administration. Ex vivo experiments demonstrated that the anchoring module increased resistance to mechanically relevant disturbances while remaining compatible with magnetic navigation and release operations. Simulation and experimental results further confirmed predictable actuation and dosing behavior under controlled experimental conditions.

Overall, the M-DCDC provides an integrated engineering framework for localized and controlled gastrointestinal drug delivery using magnetic capsule robots. Although further in vivo validation is needed, this approach represents a promising platform for advancing targeted drug delivery in minimally invasive gastrointestinal interventions.

Acknowledgments

This work is supported by the Fujian Science and Technology Project (No. 2025I0003), the Opening Project of the Key Laboratory of Bionic Engineering (Ministry of Education), Jilin University (No. KF202504), and the National Natural Science Foundation of China (Nos. U24A20525 and 82402501).

Author contributions

Shengqian QU: writing–original draft, data curation, methodology, visualization, and software. Siyuan HAN: writing–original

draft, formal analysis, software, validation, and visualization. Zitong LIAO: investigation. Wenbo ZHOU: software. Congxin JIE: visualization. Chunying LI: project administration and supervision. Shichao NIU: project administration and resources. Gang LIU: conceptualization, project administration and supervision. Shuxiang GUO: conceptualization, methodology, and writing–review and editing. Fanhong CHEN: supervision. Xiaohui DU: project administration. Yang ZHAO: funding acquisition, resources, and writing–review and editing.

Conflict of interest

Shengqian QU, Siyuan HAN, Zitong LIAO, Wenbo ZHOU, Congxin JIE, Chunying LI, Shichao NIU, Gang LIU, Shuxiang GUO, Fanhong CHEN, Xiaohui DU, and Yang ZHAO declare that they have no conflict of interest.

Declaration on the use of generative AI tools

During the preparation of this work, the authors used Qwen to improve language and readability. After using this tool, the authors reviewed and edited the content as needed and take full responsibility for the content of the publication.

Data availability

Data are available on reasonable request.

References

Bianchi F, Masaracchia A, Damone A, et al., 2022. Hybrid 6-DoF magnetic localization for robotic capsule endoscopes compatible with high-grade magnetic field navigation. *IEEE Access*, 10:4414-4430. https://doi.org/10.1109/ACCESS.2021.3136796

Cai ZC, Qin YD, Han JD, 2024. Design and control of a miniaturized magnetic-driven deformable capsule robot for targeted drug delivery. *IEEE Transactions on Industrial Electronics*, 71(8):9150-9160. https://doi.org/10.1109/TIE.2023.3314843

Cao Q, Deng RY, Pan Y, et al., 2024. Robotic wireless capsule endoscopy: recent advances and upcoming technologies. *Nature Communications*, 15(1):4597. https://doi.org/10.1038/s41467-024-49019-0

Cao Q, Pan Y, Zhang YQH, et al., 2025. A dual-functional capsule robot for drug delivery and tissue biopsy based on magnetic torsion spring technology. *Bio-Design and Manufacturing*, 8(3):495-510. https://doi.org/10.1631/bdm.2400276

Chen WY, Sui J, Wang CY, 2022. Magnetically actuated capsule robots: a review. *IEEE Access*, 10:88398-88420. https://doi.org/10.1109/ACCESS.2022.3197632

Chu JN, Traverso G, 2022. Foundations of gastrointestinal-based drug delivery and future developments. *Nature Reviews Gastroenterology & Hepatology*, 19(4):219-238. https://doi.org/10.1038/s41575-021-00539-w

Erin O, Boyvat M, Lazovic J, et al., 2021. Wireless MRI-powered reversible orientation-locking capsule robot. *Advanced Science*, 8(13):2100463. https://doi.org/10.1002/advs.202100463

Esendag K, McAlindon ME, Rus D, et al., 2024. A chemical reaction-driven untethered volume changing robotic capsule for tissue dilation. *IEEE Transactions on Medical Robotics and Bionics*, 6(4):1300-1308. https://doi.org/10.1109/TMRB.2024.3464728

Ezike TC, Okpala US, Onoja UL, et al., 2023. Advances in drug delivery systems, challenges and future directions. *Heliyon*, 9(6):e17488. https://doi.org/10.1016/j.heliyon.2023.e17488

Fu Q, Zhang X, Zhang SY, et al., 2022. A magnetically capsule robot for biomedical application. *Applied Bionics and Biomechanics*, 2022:2233417. https://doi.org/10.1155/2022/2233417

Han D, Wen RQ, Yan GZ, et al., 2025. Stable wireless power transfer system for capsule robot using three-dimensional hybrid transmitting coil pairs. *IEEE Transactions on Power Electronics*, 40(6):8824-8833. https://doi.org/10.1109/TPEL.2025.3535530

Hua DZ, Liu XH, Lu H, et al., 2022. Design, fabrication, and testing of a novel ferrofluid soft capsule robot. *IEEE/ASME Transactions on Mechatronics*, 27(3):1403-1413. https://doi.org/10.1109/TMECH.2021.3094213

Hua SS, 2020. Advances in oral drug delivery for regional targeting in the gastrointestinal tract-influence of physiological, pathophysiological and pharmaceutical factors. *Frontiers in Pharmacology*, 11:524. https://doi.org/10.3389/fphar.2020.00524

Huang L, Xie TC, Yin LR, 2025. Magnetically-actuated intracorporeal biopsy robot based on Kresling Origami. *Theoretical and Applied Mechanics Letters*, 15(1):100500. https://doi.org/10.1016/j.taml.2024.100500

Kim JS, Sung IH, Kim YT, et al., 2006. Experimental investigation of frictional and viscoelastic properties of intestine for microendoscope application. *Tribology Letters*, 22(2):143-149. https://doi.org/10.1007/s11249-006-9073-0

Kim S, Bae S, Lee W, et al., 2024. Magnetic navigation system composed of dual permanent magnets for accurate position and posture control of a capsule endoscope. *IEEE Transactions on Industrial Electronics*, 71(1):739-748. https://doi.org/10.1109/TIE.2023.3245195

Li ZZ, Wei TY, Zhang Y, et al., 2025. Rotating multibarreled capsule robot for multiple biopsies and on-demand drug delivery. *IEEE/ASME Transactions on Mechatronics*, 30(6):7089-7099. https://doi.org/10.1109/TMECH.2025.3532617

Miftahof RN, 2005. The wave phenomena in smooth muscle syncytia. *In Silico Biology*, 5(5-6):479-498. https://doi.org/10.3233/ISB-00204

Song S, Yuan SS, Zhang F, et al., 2022. Integrated design and decoupled control of anchoring and drug release for wireless capsule robots. *IEEE/ASME Transactions on Mechatronics*, 27(5):2897-2907. https://doi.org/10.1109/TMECH.2021.3125673

Sun X, Zhang P, Ye Z, et al., 2023. A soft capsule for magnetically driven drug delivery based on a hard-magnetic elastomer foam. *ACS Biomaterials Science & Engineering*,

9(12):6915-6925.
https://doi.org/10.1021/acsbiomaterials.3c00710

Valdastri P, 2025. Magnetic keys unlock multichamber capsule robots for smart interventions in the digestive tract. *National Science Review*, 12(12):nwaf486.
https://doi.org/10.1093/nsr/nwaf486

Wang M, Song S, Liu J, et al., 2021. Multipoint simultaneous tracking of wireless capsule endoscope using magnetic sensor array. *IEEE Transactions on Instrumentation and Measurement*, 70:7502510.
https://doi.org/10.1109/TIM.2021.3075776

Wang WJ, Zhang K, Ming FH, et al., 2025. A novel scheme for non-invasive drug delivery with a magnetically controlled drug delivering capsule endoscope. *Journal of Controlled Release*, 381:113591.
https://doi.org/10.1016/j.jconrel.2025.113591

Wen RQ, Yan GZ, Wang ZW, et al., 2024. Wireless power transfer system for capsule robot designed by radial square transmitting coil pair with novel ferrite structure. *The International Journal of Medical Robotics and Computer Assisted Surgery*, 20(1):e2598.
https://doi.org/10.1002/rcs.2598

Wu ZH, Wang XL, Lu Y, et al., 2025. Multichamber magnetic capsule robot for selective liquid sampling and drug delivery. *National Science Review*, 12(11):nwaf400.
https://doi.org/10.1093/nsr/nwaf400

Yang PA, Han YX, Mo CY, et al., 2025. A review and perspective of magnetic-controlled microbots for medical applications. *Chemical Engineering Journal*, 520:165814.
https://doi.org/10.1016/j.cej.2025.165814

Ye B, Shu Z, Wang SF, et al., 2025. Design and control of a dual-drug-chamber drug delivery capsule robot for multi-target drug delivery. *IEEE Transactions on Automation Science and Engineering*, 22:20759-20769.
https://doi.org/10.1109/TASE.2025.3604374

Yu XK, Wang JL, Su JR, et al., 2025. Inchworm-like biomimetic magnetic-driven robotic shell for capsule endoscope in a tubular environment. *IEEE/ASME Transactions on Mechatronics*, 30(3):2234-2244.
https://doi.org/10.1109/TMECH.2024.3435791

Zhang H, Li YH, Li Z, 2022. 6-D spatial localization of wireless magnetically actuated capsule endoscopes based on the fusion of Hall sensor array and IMU. *IEEE Sensors Journal*, 22(13):13424-13433.
https://doi.org/10.1109/JSEN.2022.3175919

Zhang H, Luo KD, Wang FH, et al., 2025. Development of a magnetically-actuated capsule robot for biopsy sampling using SMA. *Journal of Bionic Engineering*, 22(4):1609-1621.
https://doi.org/10.1007/s42235-025-00734-4

Zhang P, Chen RZ, Dong WG, et al., 2024. Robust capsule-robot positioning with limited magnetic observations: an inertial-enhanced approach. *Geo-spatial Information Science*, 27(2):475-486.
https://doi.org/10.1080/10095020.2022.2085189

Zheng LL, Guo SX, Kawanishi M, 2022. Magnetically controlled multifunctional capsule robot for dual-drug delivery. *IEEE Systems Journal*, 16(4):6413-6424.
https://doi.org/10.1109/JSYST.2022.3145869

Zheng Y, Zheng GZ, Li YY, et al., 2023. Implantable magnetically-actuated capsule for on-demand delivery. *Journal of Controlled Release*, 364:576-588.
https://doi.org/10.1016/j.jconrel.2023.11.009